JOURNAL OF MATERIALS SCIENCE **34** (1999) 2151–2157

The dielectric response of a polymeric three-component composite

G. M. TSANGARIS*, G. C. PSARRAS
National Technical University of Athens, Chemical Engineering Department, Materials Science and Engineering Section, 9 Iroon Polytechniou Str., Athens 15780
E-mail: gtsang@orfeas.chemeng.ntua.gr

The dielectric behaviour of a composite system of epoxy resin filled with Kevlar fibres and Aluminum powder is investigated in the frequency range 20 Hz to 10 MHz and the temperature interval 10 to 150 °C. Dielectric permittivity is increasing with filler content and temperature, being always higher in the low than in the high frequency range. Dielectric permittivity and loss of the composites is mostly affected by interfacial polarization arising from inhomogeneites at interfaces introduced by the fillers. Equations based on the extension of the logarithmic law of mixtures are formulated and their applicability tested with the experimental data obtained.

1. Introduction

Composite materials consisting of a polymeric matrix and conductive or non-conductive fillers are used in a variety of applications ranging from EMI shields, dissipative plastics and conductive coatings to high performance parts for aeroplane, aerospace and electronic industry [1–3].

Composite materials with three components, namely, the polymeric matrix, non conductive fibers and conductive powder can be made, thus achieving enhanced mechanical properties together with desirable conductivity.

A variety of relationships has been proposed for the calculation of the dielectric permittivity of systems with two components [4] while publications referring to systems with three components are scarce [5].

In this work relationships for the calculation of the dielectric permittivity and dielectric loss of a system with three components were developed using the extension of the logarithmic law of mixtures and their applicability tested on a system having an epoxy resin as polymer matrix with fillers Kevlar fibres and aluminum powder. The dielectric response of this three component system is also analytically discussed.

2. Proposed model

The logarithmic law of mixtures [6] written for three components can be extended to a generalised electric susceptibility parametre χ and a model can be developed to calculate the dielectric permittivity and loss of the system. Dielectric permittivity $\varepsilon^* = \varepsilon' - j\varepsilon''$ is related to the dielectric susceptibility $\chi^* = \chi' - j\chi''$ by the relationships $\chi' = \varepsilon' - 1$ and $\chi'' = \varepsilon''$ [7]. In the case of a dielectric containing conductive and non-conductive inclusions, the logarithmic law of mixtures using complex susceptibilities is written: (suffices are: 1 for the matrix, 2 for the conductive inclusions having volume fraction v and 3 for the non-conductive inclusions having volume fraction u)

$$\log \chi^* = (1-u-v)\log \chi_1^* + v\cdot\log \chi_2^* + u\cdot\log \chi_3^* \quad (1)$$

or

$$\chi^* = (\chi_1^*)^{1-v-u}(\chi_2^*)^v(\chi_3^*)^u \quad (2)$$

since

$$\chi_1^* = \varepsilon_1^* - 1 \quad \text{and} \quad \varepsilon_1^* = \varepsilon_1' - j\varepsilon_1'' \quad (3)$$

then

$$\chi_1^* = (\varepsilon_1' - 1) - j\varepsilon_1'' \quad \text{or} \quad \chi_1^* = |\chi_1^*|\exp(j\phi) \quad (4)$$

where

$$|\chi_1^*| = \left[(\varepsilon_1' - 1)^2 + (\varepsilon_1'')^2\right]^{\frac{1}{2}} \quad \text{and}$$

$$\phi = \tan^{-1}\left[\frac{\varepsilon_1''}{\varepsilon_1' - 1}\right] \quad (5)$$

Similarly

$$|\chi_2^*| = \left[(\varepsilon_2' - 1)^2 + (\varepsilon_2'')^2\right]^{\frac{1}{2}}, \quad \theta = \tan^{-1}\left[\frac{\varepsilon_2''}{\varepsilon_2' - 1}\right] \quad (6)$$

$$|\chi_3^*| = \left[(\varepsilon_3' - 1)^2 + (\varepsilon_3'')^2\right]^{\frac{1}{2}}, \quad \rho = \tan^{-1}\left[\frac{\varepsilon_3''}{\varepsilon_3' - 1}\right] \quad (7)$$

* Author to whom all correspondence should be addressed.

Finally, because $\varepsilon'' = \varepsilon' \cdot \tan\delta$

$$\chi_1^* = \left[(\varepsilon_1' - 1)^2 + (\varepsilon_1' \tan\delta_1)^2\right]^{\frac{1}{2}} \exp(j\phi) \quad (8)$$

$$\chi_2^* = \left[(\varepsilon_2' - 1)^2 + (\varepsilon_2' \tan\delta_2)^2\right]^{\frac{1}{2}} \exp(j\theta) \quad (9)$$

$$\chi_3^* = \left[(\varepsilon_3' - 1)^2 + (\varepsilon_3' \tan\delta_3)^2\right]^{\frac{1}{2}} \exp(j\rho) \quad (10)$$

Equation 9 can be transformed to

$$\chi_2^* = \varepsilon_2' \left[1 + \frac{\sigma_2^2}{(\omega \cdot \varepsilon_0)^2 (\varepsilon_2')^2}\right]^{\frac{1}{2}} \exp(j\theta) \quad (11)$$

where ω is the frequency, σ_2 the conductivity of the second constituent and ε_0 the permittivity of the free space, since

$$(\varepsilon_2' - 1)^2 \cong (\varepsilon_2')^2 \quad \text{and} \quad \tan\delta_2 = \frac{\sigma_2}{\omega\varepsilon_0\varepsilon_2'} \quad (12)$$

In the case of a conductive filler the term $\sigma_2/\omega\varepsilon_0\varepsilon_2'$ is very much greater than unity so that Equation 11 can be written as

$$\chi_2^* = \frac{\sigma_2}{\omega\varepsilon_0} \exp(j\theta) \quad (13)$$

or from Equation 12

$$\chi_2^* = \frac{\sigma_2}{\omega\varepsilon_0} \exp\left(j\frac{\pi}{2}\right) \quad (14)$$

Using Equations 8, 10 and 14, Equation 2 can be written

$$\chi^* = \left(\frac{\sigma_2}{\omega\varepsilon_0}\right)^v \cdot \left[(\varepsilon_1' - 1)^2 + (\varepsilon_1' \tan\delta_1)^2\right]^{\frac{1-v-u}{2}} \cdot \left[(\varepsilon_3' - 1)^2 + (\varepsilon_3' \tan\delta_3)^2\right]^{\frac{u}{2}} \cdot \exp j\left[\frac{\pi v}{2} + \rho u + \phi(1 - v - u)\right] \quad (15)$$

From this equation since

$$\mathrm{Re}\chi^* = \varepsilon' - 1 \quad \text{and} \quad \mathrm{Im}\chi^* = \varepsilon'' \quad (16)$$

the following relationships are obtained:

$$\varepsilon' = \left(\frac{\sigma_2}{\omega\varepsilon_0}\right)^v \cdot \left[(\varepsilon_1' - 1)^2 + (\varepsilon_1' \tan\delta_1)^2\right]^{\frac{1-v-u}{2}} \cdot \left[(\varepsilon_3' - 1)^2 + (\varepsilon_3' \tan\delta_3)^2\right]^{\frac{u}{2}} \cdot \cos\left[\frac{\pi v}{2} + \rho u + \phi(1 - v - u)\right] + 1 \quad (17)$$

$$\varepsilon'' = \left(\frac{\sigma_2}{\omega\varepsilon_0}\right)^v \cdot \left[(\varepsilon_1' - 1)^2 + (\varepsilon_1' \tan\delta_1)^2\right]^{\frac{1-u-v}{2}} \cdot \left[(\varepsilon_3' - 1)^2 + (\varepsilon_3' \tan\delta_3)^2\right]^{\frac{u}{2}} \cdot \sin\left[\frac{\pi v}{2} + \rho u + \phi(1 - v - u)\right] \quad (18)$$

To take into account the dependence of the geometric characteristics of the inclusions Equations 17 and 18 must be modified again using the logarithmic law of mixtures.

The real and imaginary parts of the system's susceptibility χ'_{mod}, χ''_{mod} respectively, can be resolved into two components, parallel and normal to the electric field. Susceptibility is directly related to the polarization produced by the electric field and changes in polarization are reflected in the susceptibility and permittivity of the system. It can then be written that

$$\chi'_{\mathrm{mod}} \cong (\chi')^{Y_\parallel} (\chi')^{Y_\perp} \quad (19)$$

$$\chi''_{\mathrm{mod}} \cong (\chi'')^{Y_\parallel} (\chi'')^{Y_\perp} \quad (20)$$

In Equations 19 and 20 $Y_\parallel$ and $Y_\perp$ are quantities depending on the geometric characteristics of the inclusions and correspond to the part of polarization oriented parallel and normal to the electric field respectively. However the intensity of dielectric phenomena is more evident along the axis of the ellipsoidal inclusions parallel to the electric field than in the normal direction [8, 9] and Equations 19 and 20 can easily, be transformed to

$$\varepsilon'_{\mathrm{mod}} = A\left[(\varepsilon' - 1)^Y + 1\right] \quad (21)$$

$$\varepsilon''_{\mathrm{mod}} = B(\varepsilon'')^Y + C \quad (22)$$

In Equations 21 and 22 $Y_\parallel$ has been replaced by Y the depolarizing factor [10] which depends on the aspect ratio and the orientation of the inclusions [11].

It is given [12, 13] by

$$Y_1 = \frac{1}{1 - (a/b)^2} - \frac{a/b}{[1 - (a/b)^2]^{\frac{3}{2}}} \cos^{-1}(a/b) \quad (23)$$

for $a < b$, where a/b is the aspect ratio and by

$$Y_2 = \left[\ln\left(\frac{2a}{b}\right) - 1\right]\left(\frac{b}{a}\right)^2 \quad (24)$$

for $a > b$. Y_1 is valid for the metal particles [14] while Y_2 for the fiber inclusions [15]. The effects of the presence of both kind of inclusions in the matrix are taken into account by replacing Y in Equations 21 and 22 with the sum $Y_1 + Y_2$ so that Equations 21 and 22 are rewritten as

$$\varepsilon'_{\mathrm{mod}} = A\left[(\varepsilon' - 1)^{Y_1+Y_2} + 1\right] \quad (25)$$

$$\varepsilon''_{\mathrm{mod}} = B(\varepsilon'')^{Y_1+Y_2} + C \quad (26)$$

Constants A, B, C are related to the behaviour of the system at the boundary conditions.

Neglecting the terms $(\varepsilon_1' \tan\delta_1)^2$, $(\varepsilon_3' \tan\delta_3)^2$ because they are very small, the parameters A, B, C in Equations 25, 26 are calculated from the following boundary conditions.

For $v = 0$ and $u = 0$,

$\varepsilon'_{\mathrm{mod}} = \varepsilon_1'$, $\varepsilon' = \varepsilon_1'$

$\varepsilon''_{\mathrm{mod}} = \varepsilon_1''$, $\varepsilon'' = \varepsilon_1''$, parameters A, C are thus obtained.

For $v = 1$,

$$\varepsilon''_{\text{mod}} = \varepsilon''_2, \quad \varepsilon''_2 = 0 \quad \text{and } B \text{ is obtained.}$$

The expressions for A, B, and C are

$$A = \frac{\varepsilon'_1}{\left[(\varepsilon'_1 - 1)^{Y_1+Y_2} + 1\right]},$$
$$B = \varepsilon''_1 \left(\frac{\omega\varepsilon_0}{\sigma_2}\right)^{Y_1+Y_2}, \quad C = \varepsilon''_1 \tag{27}$$

Using Equations 27, Equations 25 and 26 acquire their final form

$$\varepsilon'_{\text{mod}} = \frac{\varepsilon'_1}{\left[(\varepsilon'_1 - 1)^{Y_1+Y_2} + 1\right]} \left\{ \left[\left(\frac{\sigma_2}{\omega\varepsilon_0}\right)^{v} \times (\varepsilon'_1 - 1)^{1-v-u} (\varepsilon'_3 - 1)^{u} \cos \times \left[\pi \frac{v}{2} + \rho u + \phi(1 - v - u) \right] \right]^{Y_1+Y_2} + 1 \right\} \tag{28}$$

$$\varepsilon''_{\text{mod}} = \varepsilon''_1 \left\{ \left[\left(\frac{\sigma_2}{\omega\varepsilon_0}\right)^{v-1} (\varepsilon'_1 - 1)^{1-v-u} (\varepsilon'_3 - 1)^{u} \sin \times \left[\pi \frac{v}{2} + \rho u + \phi(1 - v - u) \right] \right]^{Y_1+Y_2} + 1 \right\} \tag{29}$$

Equations 28, 29 and 23, 24 constitute the proposed model for the evaluation of dielectric behaviour of a composite consisting of a polymeric matrix with conductive and non conductive inclusions.

Permittivity and loss of the matrix (ε'_1, ε''_1) and the filler (ε'_3, ε''_3) the conductivity of the metal particles σ_2, and the aspect ratio of all inclusions must be known [14, 15, 22].

3. Experimental

To test the equations describing the dielectric behaviour of a composite having both conductive and non conductive inclusions a number of specimens consisting of an epoxy resin, aluminum particles and kevlar fibres were used.

The epoxy resin was a commercially available bisphenol type (Epikote 828, Shell Co.) and it was used as a prepolymer having molecular weight ∼320 and viscosity 25000 MPa · s at 25 °C. As curing agent triethylene tetramine at 8 phr (parts of curing agent per hundred parts of resin) was employed. The product KEVLAR 49 aramid pulp of E. I. Du Pont de Nemours was used as filler which had the following properties: mean length of fibres 2 mm, diameter ∼14 μm and density 1.44 g/cm^3 [16]. Before use it was dried at 100 °C for 2 h. Aluminum powder (Merck) was also used as filler which consisted of ellipsoidal particles with a mean aspect ratio $a/b = 100/115 = 0.87$. Composites with 0, 0.5, 1.0, 1.5 phr in kevlar fibres and aluminum powder 0, 5, 15, 25 phr were prepared. For every content of aluminum powder in the epoxy resin four specimens were prepared with the above varying content in kevlar fibres.

The preparation was carried out as follows: The epoxy prepolymer was heated at 60 °C and then distilled acetone containing the required kevlar pulp quantity was added to the resin. The mixture was heated to 130 °C to remove acetone, then cooled freely to 60 °C and the curing agent was added. Afterwards the required quantity of aluminum powder was added and continuous stirring was employed. The composite was then poured into suitable plexiglass moulds. Initial curing was carried out at ambient for 24 h, followed by post curing at 100 °C for 48 h.

Specimens in circular disk form 60 mm in diameter and 3 mm thick were produced by machining from the original castings. Satisfactorily homogeneous composites were produced exhibiting no visible flaws or voids. Faces of specimens were painted with silver paint to improve contact and were stored in a vacuum desiccator in the presence of silica gel for at least 5 days before measurement to avoid any influence of moisture.

Dielectric measurements were performed using a video-bridge (T2100 of Electro Scientific Instruments Co.) in the frequency range 20 Hz to 20 kHz and an impedance analyzer (4192A of Hewllet Packard) in the frequency range 20 kHz to 10 MHz. The test cell was a three terminal guarded system according to ASTM D150-92 and D257-91 specifications. Details of the cell are given elsewhere [17].

4. Results

The dielectric permittivity ε' versus frequency for the composites with either constant kevlar content and varying amount of A1 particles or constant A1 particles content and varying amount of kevlar fibres are shown in Fig. 1a, b at the temperature of 40 °C and in Fig. 2a, b at the temperature of 120 °C.

Dielectric permittivity increases as the content of the conductive phase is raised Fig. 1a. Permittivity values are higher at higher temperatures in the whole frequency range. However at elevated temperatures and in the low frequency regime, permittivity values become even higher indicating a relaxation process Fig. 2a.

The non-conductive constituent shows a weak influence on the permittivity of the composite Figs 1b and 2b. Dielectric loss of the composites versus frequency are shown in Figs 1c, d and 2c, d. As the conductive phase increases, dielectric losses also increase (1c). At the low frequency range relaxation peaks tend to be formed Fig. 1c, and are clearer at the temperature of 120 °C, Fig. 2c. Increasing the content of the conductive filler, peaks are moving to lower frequencies. At the other end of frequency spectrum losses are also increasing and another relaxation tends to be formed.

The dielectric permittivity ε' versus temperature of the composites already described is shown in Figs 3 and 4 for the frequency of 1 kHz and 1 MHz respectively. A slight increase in permittivity with temperature is observed, which at elevated temperatures near T_g, becomes more evident. The dependence of dielectric permittivity from temperature is more intense in

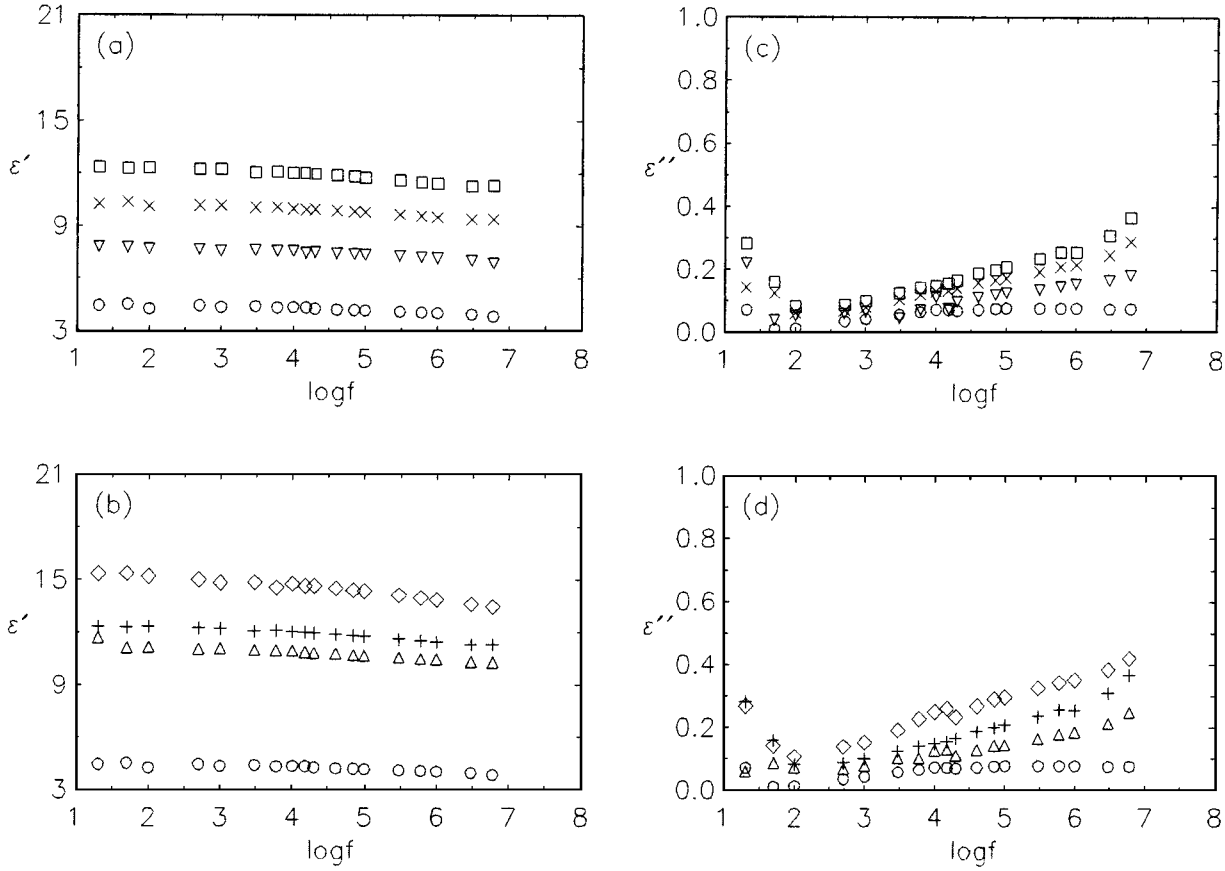

Figure 1 Dielectric permittivity (ε') and loss (ε'') versus frequency at the temperature of 40 °C for the specimens: (a), (c) with constant Kevlar content 1 phr and varying Al particles (○ pure epoxy, ∇ 5 phr Al, × 15 phr Al, □ 25 phr Al), (b), (d) with constant Al content 25 phr and varying amount of Kevlar fibres (○ pure epoxy, Δ 0.5 phr Kevlar, +1.0 phr Kevlar, ◊ 1.5 phr Kevlar).

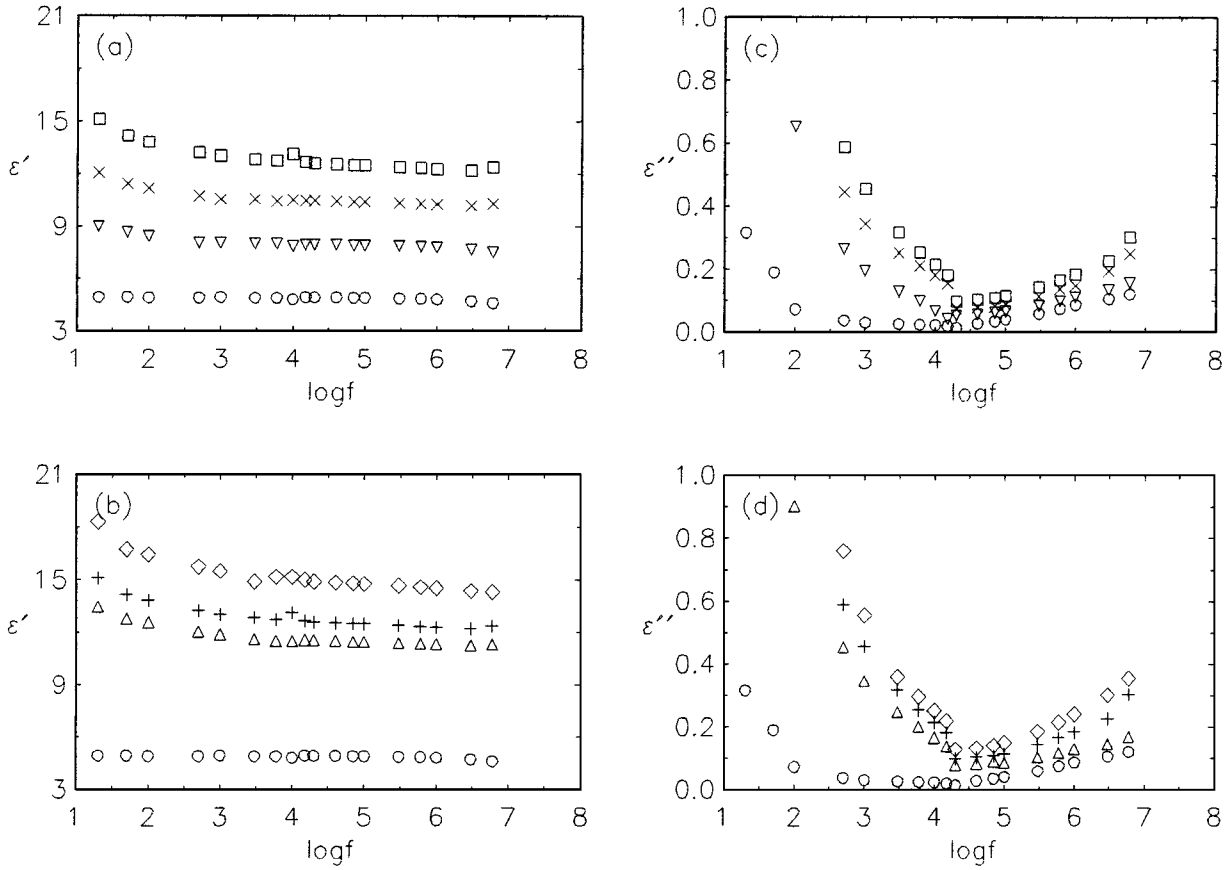

Figure 2 Dielectric permittivity (ε') and loss (ε'') versus frequency at the temperature of 120 °C for the specimens: (a), (c) with constant Kevlar content 1 phr and varying Al particles (○ pure epoxy, ∇ 5 phr Al, × 15 phr Al, □ 25 phr Al), (b), (d) with constant Al content 25 phr and varying amount of Kevlar fibres (○ pure epoxy, Δ 0.5 phr Kevlar, +1.0 phr Kevlar, ◊ 1.5 phr Kevlar).

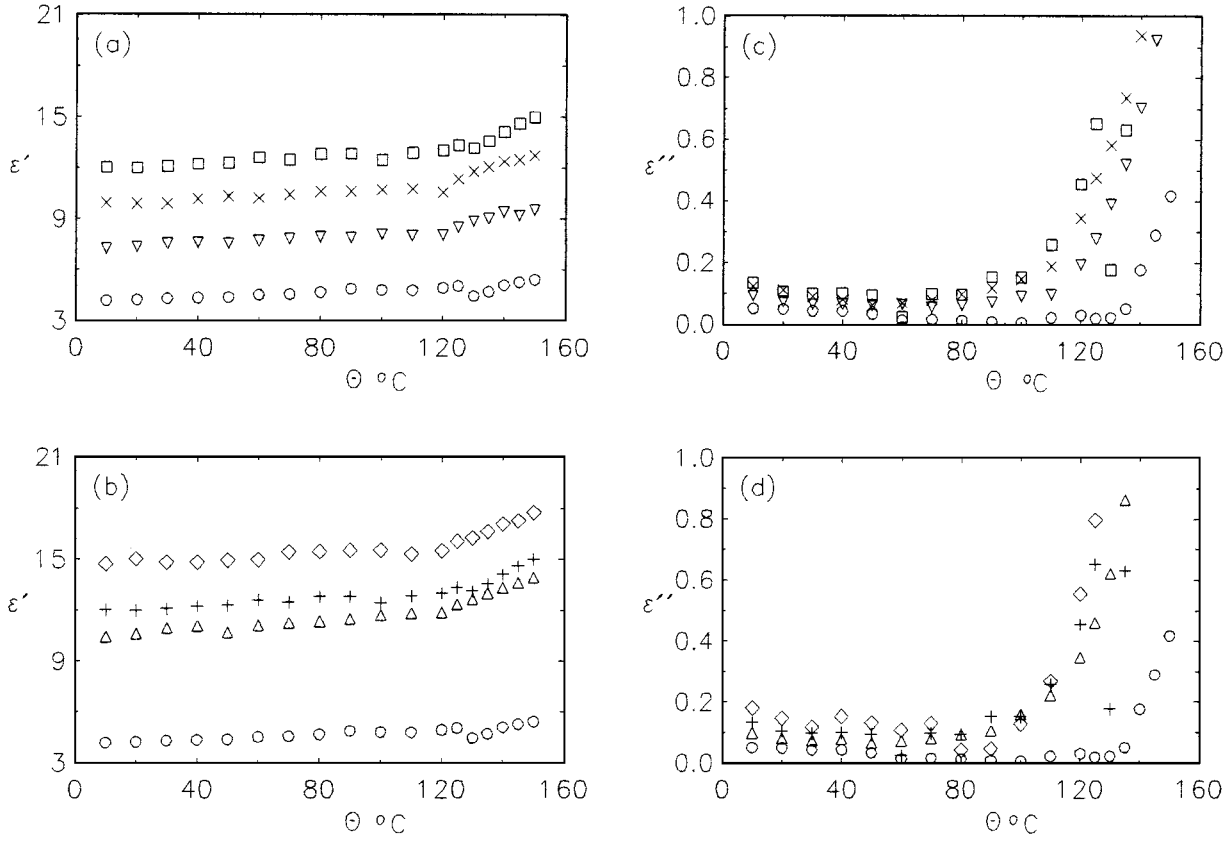

Figure 3 Dielectric permittivity (ε') and loss (ε'') versus temperature for the specimens described in Figs 1 and 2 at the frequency of 1 kHz.

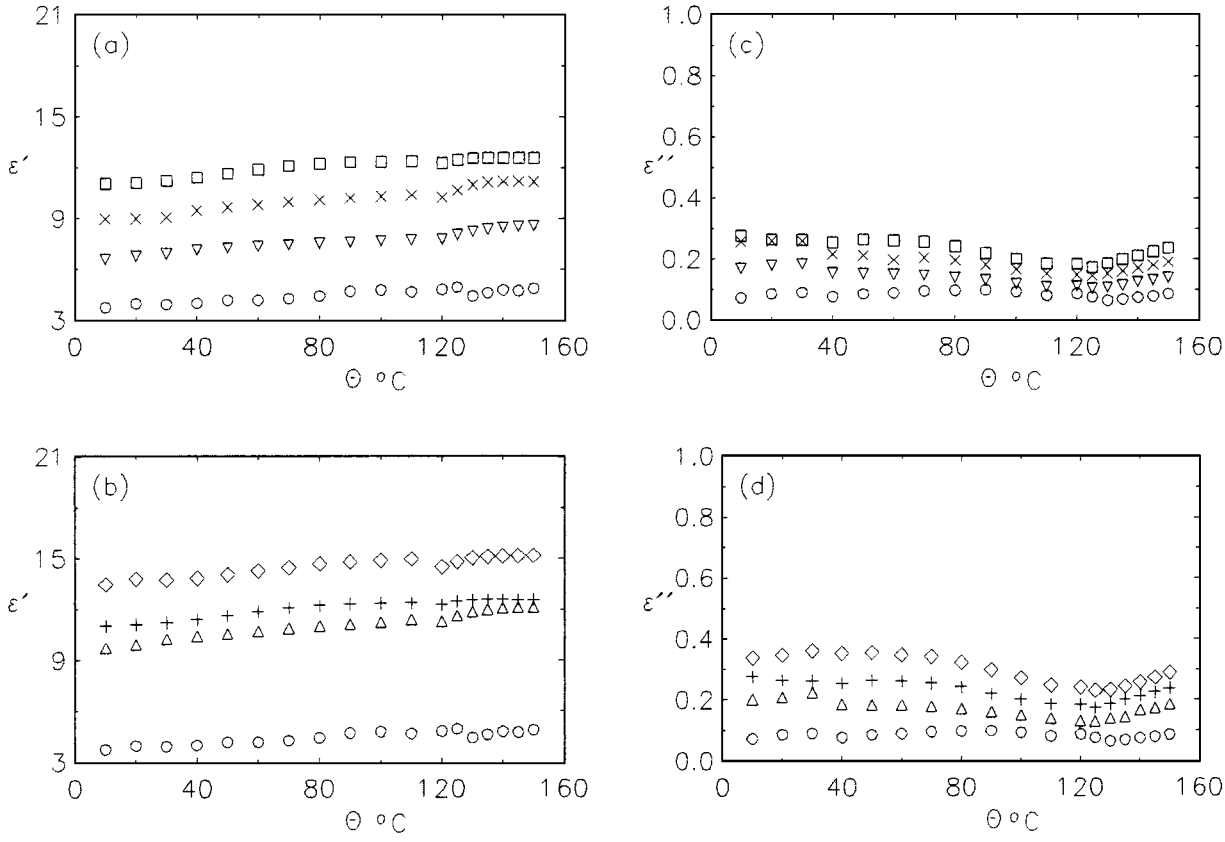

Figure 4 Dielectric permittivity (ε') and loss (ε'') versus temperature for the specimens described in Figs 1 and 2 at the frequency of 1 MHz.

the low frequencies and for high values of the fillers content (Fig. 3a, b).

Dielectric loss of the composites versus temperature is shown in Figs 3c, d and 4c, d, for the frequency of 1 kHz and 1 MHz respectively.

At low frequencies and elevated temperatures near T_g (Fig. 3c, d) peaks are formed and become higher with greater content of the conductive filler. With increasing frequency peaks are moving and disappear into the high frequency spectrum (Fig. 4c, d).

5. Discussion

The presence of the Aluminum particles increases the conductivity of the composites and consequently the permittivity acquires higher values than those of the pure epoxy matrix as predicted by theory [18] and was also experimentally found [19–21]. Figs 1a, b and 2a, b.

The weak dependence of ε' from the non-conductive filler concentration is due to the moderate heterogeneity of the systems since permittivities of the epoxy resin and kevlar fibres exhibit close values [22, 23]. At elevated temperatures permittivities are higher because of the increased segmental mobility of the matrix. Concerning the frequency dependence of ε' for filled specimens and pure epoxy, the decrease in permittivity with increasing frequency is more clear at elevated temperatures and low frequencies. In the case of a polymeric matrix a decrease in dipolar polarization can be regarded responsible for this behaviour, but in the composite systems besides the dipolar polarization of polar groups another affecting term is present, the interfacial or Maxwell-Wagner-Sillars, polarization due to the heterogeneity of the systems [24–26].

The increase in dielectric permittivity with increasing temperature can be regarded as the result of activation of two competing mechanisms. Segmental mobility of the polymer molecules increases leading to higher values of dielectric permittivity as the alignment of dipoles parallel to the field is facilitated. At the same time, differential thermal expansion of the epoxy resin and the metal disrupts the chains of the conductive metallic particles, causing a decrease in dielectric permittivity. At elevated temperatures the segmental mobility of the polymeric matrix is the dominating factor causing the permittivity to increase. Figs 3a, b and 4a, b.

Dielectric losses Figs 1c, f and 2c, d are high in the low frequency range because of the interfacial polarization. Interfacial polarization induces a Debye type dielectric relaxation [27] and the relaxation peaks shift to lower frequencies as the volume fraction of the inclusions increases [17]. Dielectric losses diminish rapidly with increasing frequency [28] because interfacial polarization related to large dipoles across interfaces is no longer active as the electric field changes direction with increasing rapidity. At the temperature of 120 °C in the high frequency range an increase of the dielectric losses and the onset of a relaxation peak can be observed, which is attributable to β relaxation process [21] resulting from the residue amine groups of the curing agent or the hydroxyl groups formed by the epoxy ring opening. Fig. 2c.

Scanning dielectric losses with temperature at constant frequency (1 kHz) the α-relaxation peak starts to be formed at high temperatures near T_g of the epoxy resin matrix, as mobility of large parts of polymer molecules is enhanced. At higher frequencies (1 MHz) maxima shift to higher temperatures because increased temperature results in faster movement leading to decreased relaxation times, with the consequent shift of maxima to higher frequencies. Figs 3c, d and 4c, d. To test the applicability of the proposed model on the

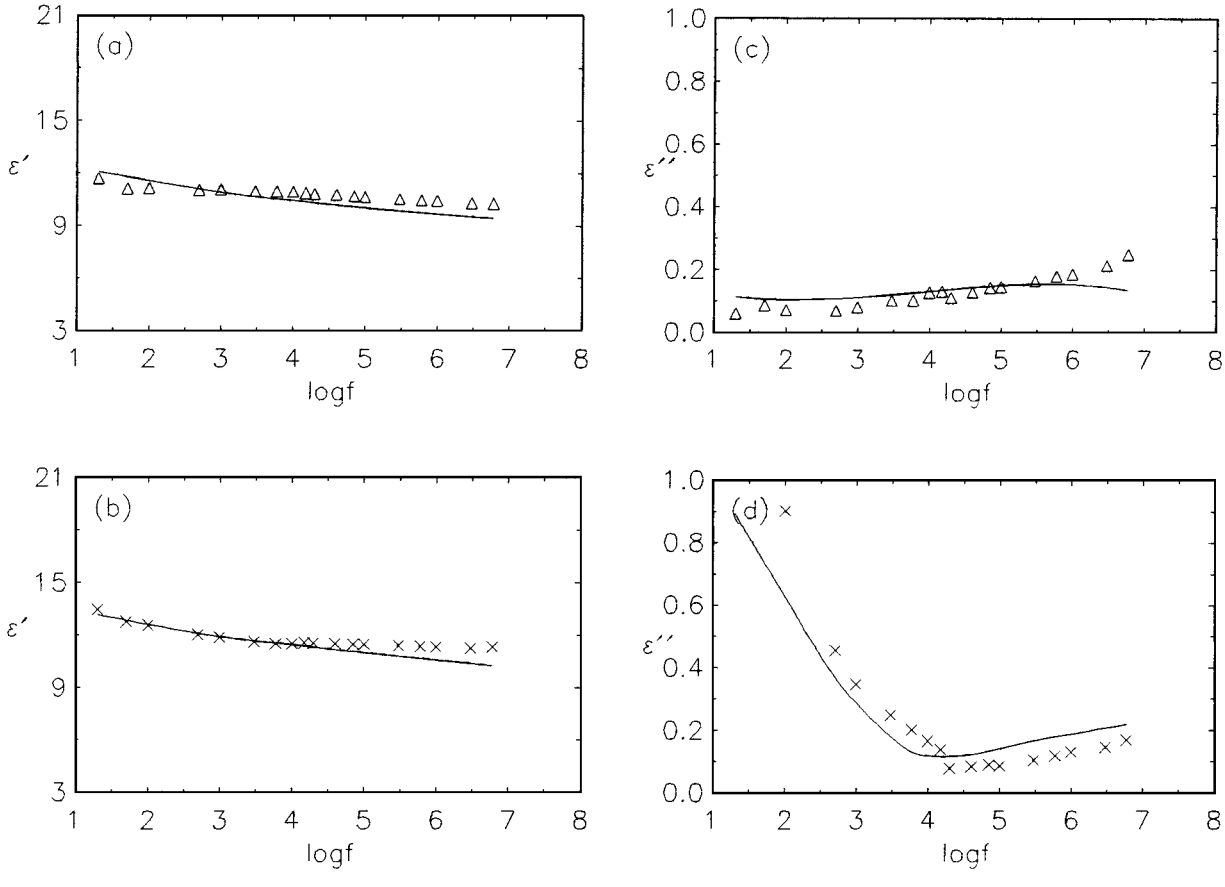

Figure 5 Dielectric permittivity (ε') and loss (ε'') versus frequency of the composite with volume fractions $v = 0.093$ (25 phr Al) and $u = 0.004$ (0.5 phr Kevlar), at the temperatures of 40 °C (a), (c) and 120 °C (b), (d). Continuous lines represent values given by model, symbols represent experimental values.

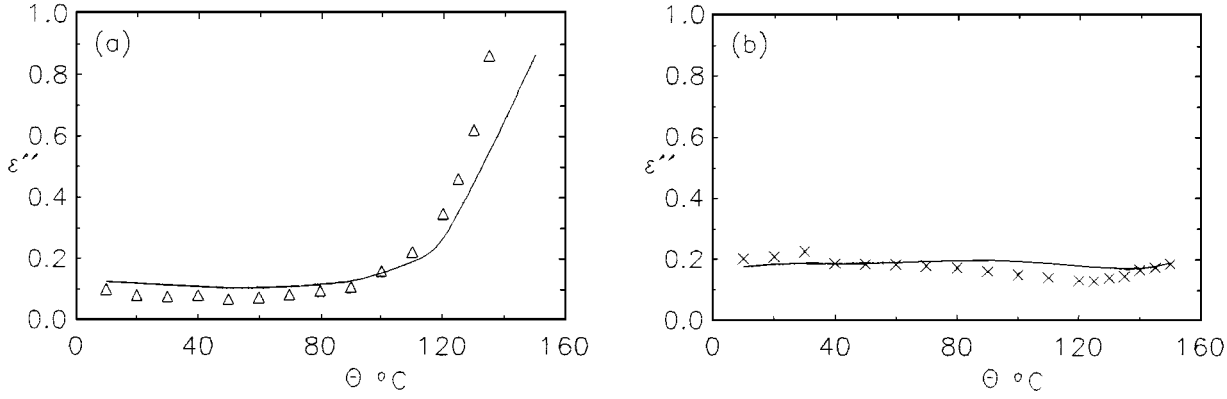

Figure 6 Dielectric losses (ε'') versus temperature of the composite with volume fractions $v = 0.093$ (25 phr Al) and $u = 0.004$ (0.5 phr Kevlar), at the frequencies of 1 kHz (a) and 1 MHz (b). Continuous lines represent values given by model, symbols represent experimental values.

described dielectric behaviour of the composites with three components, the dielectric permittivity and dielectric loss of the composites were calculated using Equations 23, 24 and 28, 29 and were compared with experimental values from Figs 1–4.

In Fig. 5 calculated values of dielectric permittivity and loss versus frequency are presented together with experimental ones from Figs 1b, d and 2b, d, for two temperatures namely 40 and 120 °C for representative composites with volume fraction for Al $v = 0.093$ (25 phr) and for Kevlar fibers $u = 0.004$ (5 phr).

In Fig. 6 calculated values of dielectric permittivity and loss versus temperature of the same composites together with experimental ones from Figs 3b, d and 4b, d are presented for two frequencies namely 1 kHz and 1 MHz.

The proposed model satisfactorily follows the dielectric behaviour of the composites described above and depicts all changes of permittivity and loss occuring by the changes of frequency or temperature or volume fraction. Deviation from the experimental values must be attributed to the intrinsic weakness of the logarithmic law of mixtures on which the model is based. However an improvement to the approximation of the part of polarization oriented parallel and normal to the electic field can result to an even more satisfactory performance of the specific model.

6. Conclusions

The dielectric response of a polymeric three component composite can be described by a set of four equations derived through the logarithmic law of mixtures. The proposed equations satisfactorily depict changes in permittivity and dielectric losses induced by variations in frequency, temperature, the volume fraction of the inclusions and their geometrical characteristics.

References

1. R. P. SHELDON, "Composite Polymeric Materials" (Applied Science Publishers, London, 1982) p. 185.
2. M. M. SCHWARTS, "Composite Materials Handbook" (McGraw-Hill, New York, 1984) p. 3.81.
3. J. DELMONTE, "Metal/Polymer Composites" (Van Nostrand Reinhold, New York, 1990) pp. 40, 65.
4. B. TAREEV, "Physics of Dielectric Materials" (Mir Publishers, Moscow, 1975) p. 123.
5. S. RADHAKRISHNAN, *J. Mater. Sci. Lett.* **4** (1985) 1445.
6. K. LICHTENECKER and K. ROTHER, *Phys. Z.* **32** (1931) 255.
7. A. CHELKOWSKI, "Dielectric Physics" (Elsevier, Amsterdam, 1980) p. 1.
8. R. W. SILLARS, *Proc. R. Soc. (London)* **A169** (1939) 66.
9. C. T. O'KONSKI, *J. Phys. Chem.* **64** (1960) 605.
10. B. K. P. SCAIFE, "Principles of Dielectrics" (Oxford University Press, Oxford, 1989) p. 291.
11. L. E. NIELSEN, *J. Phys. D, Appl. Phys.* **7** (1974) 1549.
12. P. HEDVIC, "Dielectric Spectroscopy of Polymers" (Adam Hilger, Bristol, 1977) p. 287.
13. L. K. H. VAN BECK, in "Progress in Dielectrics," Vol. 7, edited by J. B. Birks (Heywood Books, London, 1967) p. 81.
14. G. M. TSANGARIS, G. C. PSARRAS and N. KOULOUMBI, *Mater. Sci. Technol.* **12** (1996) 533.
15. *Idem. Adv. Comp. Lett.* **4** (6) (1995) 175.
16. E. I. DU PONT DE NEMOURS & CO. (Inc.), Product Data Sheet, 1986.
17. G. M. TSANGARIS, G. C. PSARRAS and A. J. KONTOPOULOS, *J. Non-Cryst. Solids* **131–133** (1991) 1164.
18. C. J. F. BÖETTCHER and P. BORDEWIJK, "Theory of Electric Polarization," Vol. 2 (Elsevier, Amsterdam, 1978) p. 476.
19. S. A. PAIPETIS, G. M. TSANGARIS and J. M. TSANGARIS, *Polym. Commun.* **24** (1983) 373.
20. R. L. MC CULLOUGH, *Comp. Sci. Technol.* **22** (1983) 3.
21. V. BAZIARD, S. BRETON, S. TOUTAIN and A. GOURDENNE, *Eur. Polym. J.* **24** (1988) 521.
22. ASM Engineering Materials Handbook, Vol. I, "Composites" (ASM International, 1987) p. 361.
23. R. BARTNIKAS and R. M. EICHHORN, ASTM Special Technical Publication 783, 1983, Vol. IIA, p. 608.
24. J. C. MAXWELL, "Electricity and Magnetism," Vol. 1 (Clarendon Press, Oxford, 1892) p. 452.
25. K. W. WAGNER, *Archs. Elektrotechnol.* **2** (1914) 378.
26. R. W. SILLARS, *J. Inst. Electr. Eng.* **80** (1937) 378.
27. G. M. TSANGARIS, N. KOULOUMBI and S. KYVELIDIS, *Mater. Chem. Phys.* **44** (1996) 245.
28. A. R. VON HIPPEL, "Dielectrics and Waves" (Wiley, New York, 1954) p. 228.

Received 29 July
and accepted 15 October 1998